Applied Surface Science 332 (2015) 89–96

Contents lists available at ScienceDirect

Applied Surface Science

journal homepage: www.elsevier.com/locate/apsusc

Adsorption of alginate and albumin on aluminum coatings inhibits adhesion of *Escherichia coli* and enhances the anti-corrosion performances of the coatings

Xiaoyan He, Yi Liu, Jing Huang, Xiuyong Chen, Kun Ren, Hua Li*

Key Laboratory of Marine Materials and Related Technologies, Zhejiang Key Laboratory of Marine Materials and Protective Technologies, Ningbo Institute of Materials Technology and Engineering, Chinese Academy of Sciences, Ningbo 315201, China

ARTICLE INFO

Article history:
Received 18 October 2014
Received in revised form
23 December 2014
Accepted 19 January 2015
Available online 27 January 2015

Keywords:
Adsorption
Aluminum coating
Alginate
Albumin
Bacterial adhesion
Corrosion

ABSTRACT

Thermal-sprayed aluminum coatings have been extensively used as protective layers against corrosion for steel structures in the marine environment. The corrosion usually deteriorates from marine biofouling, yet the mechanism of accelerated corrosion of the coatings remains elusive. As the first stage participating in biofouling process, adsorption of molecules plays critical roles in mediating formation of biofilm. Here, we report at molecular level the adsorption behaviors of albumin and marine polysaccharide on arc-sprayed aluminum coatings and their influence on adhesion of *Escherichia coli*. The adsorption of alginate and albumin was characterized by infrared spectra analyses and atomic force microscopic observation. The adsorption inhibits effectively adhesion of the bacteria. Further investigation indicates that alginate/albumin altered the hydrophilicity/hydrophobicity of the coatings instead of impacting the survival of the bacteria to decline their adhesion. The conditioning layer composed of the molecules enhances anti-corrosion performances of the coatings.

1. Introduction

Corrosion is one of the major problems encountered by marine infrastructures, and a variety of strategies, in particular, surface coating technology have been developed for marine applications. Among the cost-effective coating techniques, thermal spray has been proved to be competitive in depositing corrosion-resistant coatings for marine steel structures by providing maintenance-free protection for over 20 years [1–3]. Due to the complex nature of the marine environment, marine and offshore corrosion is predominately related to electrochemistry, which has been well established [4]. As another key concern for the marine environment, biofouling has multiple impacts on corrosion [5]. Biofilm formed as a result of biofouling promotes/inhibits corrosion of metals by a number of mechanisms, such as cathodic and anodic depolarization [6], hydrogen production [7], production of corrosive metabolites such as organic acids and exopolymers [8]. Biofouling in marine is a complex phenomenon involving more than 4000 species of marine organisms [9,10], causing serious problems such as accelerated corrosion, transport of non-native invasive species and decreased fuel efficiency [10–12]. Therefore, extensive research efforts have been devoted to clarifying the mechanisms of biofouling with an aim to prevent marine organisms from attaching onto the surfaces of the marine structures [13,14]. Yet, control and eradication of biofilms are difficult since their resistance toward most antibiotics and biocides is substantially increased [15].

Construction of antifouling coatings predominately pertains to use of polymer-based materials [16,17]. To the best knowledge of the authors, there are so far no available scientific reports focusing on influence of biofouling on anti-corrosion performances of thermal-sprayed inorganic marine coatings. The mechanism as to how biofouling affects the performances of thermal-sprayed coatings in the marine environment remains unclear. It is usually believed that biofouling involves four stages [18,19]. Adsorption of the organics such as polysaccharides and/or proteins takes place primarily in the overall biofouling [19]. The absorbance is mediated by Brownian motion, Van der Waals force, hydrogen bond and/or electrostatic interaction, forming a conditioning layer usually in a few minutes and subsequently accumulating within several hours [20,21]. On the subsequent stages, formation of microbial layer with cross-linked structure [22] and following colonization of spores of macroalgae or protozoa and larvae of macrofoulers lead to severe biofouling [23,24]. Chemistry and surface structure of the materials/coatings are the leading variables responsible for the

* Corresponding author. Tel.: +86 574 86686224; fax: +86 574 86685159.
E-mail address: lihua@nimte.ac.cn (H. Li).

http://dx.doi.org/10.1016/j.apsusc.2015.01.141
0169-4332/

biofouling, hence biofouling-enhanced corrosion [24,25]. In fact, biofouling is a complex process. Some researchers pointed out in a recent publication that biofouling does not always follow the four-stage succession model [26]. The conditioning layer is not necessarily required for biofouling. Yet, the biofilm created by bacteria/diatoms is particularly influenced by the intrinsic features of absorbed biomacromolecules. To construct anti-fouling coatings, it is still essential to understand at molecular level the adsorption behaviors of the polysaccharides/proteins and their effect on subsequent processes.

Study on vanadium pentoxide coating by Natalio et al. [27] showed that the coating functioned as vanadium halogenated peroxide, inhibiting effectively biological attachment by killing bacteria adhered initially, thus there was no microbial layer formed. This finding agrees well with the mechanism that biofouling is based on formation of biofilm [19]. However, the question still remains whether conditioning layer is necessary for development of biofilm. Conditioning layer usually consists of biomacromolecules such as polysaccharides, glycoproteins and proteins [28]. Influence of biomacromolecules on the biofilm created by bacteria and diatom is particularly dependent on the intrinsic features of the biomacromolecules. For instance, fibronectin could promote adhesion of bacteria [29], while gelatin and pepsin could inhibit the adhesion of bacteria [30]. It was proposed that attachment of bacteria and diatom would occur most readily on the surfaces coated by surface conditioning films [21]. Experimental proofs are yet needed to elucidate the mechanisms.

As typical rod-shaped bacterium, *Escherichia coli* (*E. coli*) causes serious biofouling in various environments especially for fabric and medical devices [31] and its pronounced influence on marine biofouling was reported [32]. *E. coli* shares similar properties with most marine bacteria and it was extensively studied for marine environment [33,34]. Polysaccharides and proteins are the major component of a conditioning layer. Sodium alginate widely exists in several of well-known algae and bacteria [35,36] and albumin has been chosen as typical protein for biofouling research [37]. In this paper, albumin/alginate was employed as the typical biomacromolecules to build a simplified model representing a conditioning layer. The extensively used arc-sprayed aluminum coatings were selected as the matrix materials for investigating the impact of alginate and albumin adsorbed on the coating surfaces on behaviors of *E. coli*. The adsorption behaviors of sodium alginate and albumin on the corrosion-resistant aluminum coatings in artificial sea water were characterized in situ by atomic force microscopy and infrared spectroscopy. Effect of adsorption of the polysaccharide/protein on the subsequent formation of biofilm in terms of adhesion of the bacteria and the anti-corrosion performances of coatings were elucidated.

2. Materials and experimental setup

The aluminum coatings were deposited by high-velocity arc spray (AS, TLAS-500C, China). For the spraying, the current and voltage of the arc were set at 80–100 A and 25 V, respectively, and the spray distance was 15 cm. The compressed air with the pressure of 0.5 MPa was used for the arc spraying [38]. The coatings with the thickness of ~150 μm were deposited on 316L substrate of 20 mm × 20 mm × 2 mm in dimension. For comparison purpose, some of the coatings were sealed by tetrafluoroethylene-hexafluoropropylene copolymer (FEP) and some were surface-polished to the surface roughness (Ra) of <100 nm.

Microstructural features of the coatings were examined by field emission scanning electron microscopy (FESEM; FEI Quanta FEG 250, the Netherlands). Wettability of the coating samples was determined by measuring the contact angle of deionized distilled water droplet spreading on their surfaces using a contact angle measurement instrument (Dataphysics OCA20, Germany). Surface roughness of the coatings was measured with a surface profiler, a scanning mechanical microscope (Alpha-Step IQ, KLA-Tencor, USA) with a vertical resolution of 0.012 Å. The measurement was taken by using an inductive sensor equipped with a diamond stylus probe with a pyramidal shape of 5 μm in radius and a vertex angle of 60°. A scan length of 1000 μm with a scan speed of 50 μm/s was used.

Artificial seawater (ASW) was prepared according to ASTM D1141-98. All the reagents and solvents were used as-received without any further purification. Prior to being immersed in ASW, the surface-polished 316L plates, the as-sprayed Al coating, the sealed Al coating and the surface-polished Al coating were washed by sonication in ethanol for 30 min and following three times in deionized water for 5 min at room temperature. Then the samples were soaked in 4 ml ASW containing 1 mg/ml sodium alginate (AR, Sinopharm Chemical Reagent Co. Ltd., China) and 1 mg/ml bovine serum albumin (BSA, 98% purity, Sigma-Aldrich). The samples soaked for 12 h were then rinsed twice in deionized water for 5 min followed by drying by flowing air at 37 °C. The absorbed polysaccharide/protein on the surfaces of the samples was further characterized by Fourier transform reflection adsorption infrared spectroscopy (FT-RAIRS, Varian 610-IR, USA). The infrared spectrum with a resolution of 8 cm^{-1} and the scan number of 4 was adopted with the scan range 800–4000 cm^{-1}.

It is known that adsorption behaviors of the protein/polysaccharide might be different on the surfaces of different materials. Yet, once adsorption occurs, the molecules usually exhibit similar conformational changes, in turn ensuring following interaction of other microorganisms with the adsorbed molecules. Since the observation of the morphology of alginate/albumin could be interfered by the flaws of the arc-sprayed Al coatings, for example, microsized pores, etc., silicon wafers were chosen as the matrix for acquiring the images of the absorbed molecules. The morphology information of albumin/alginate absorbed on silicon wafer can be well related to that for the Al coatings. After 10 min immersion of silicon wafers in the alginate-/albumin-containing ASW, the morphology of the absorbed alginate/albumin in liquid phase was characterized by atomic force microscopy (AFM; Agilient5500, USA). The zeta potentials of alginate and albumin with the concentration of 1 mg/ml in ASW were measured by dynamic light scattering (DLS; Zetasizer Nano ZS, UK).

Gram-negative *E. coli* bacteria (ATCC25922) were selected for the adhesion testing. The bacteria were cultured in LB media. The medium was prepared by dissolving 10 g NaCl, 5 g yeast extract and 10 g peptone in 1000 ml deionized water. The media containing the bacterial strains were shaken for 24 h at 37 °C. Nutrient agar culture medium was also used in this study. The agar medium was prepared by dissolving 38 g nutrient agar culture (Tianhe Microbial Sci. Tech. Co., Ltd., China) in 1000 ml of deionized water, followed by 120 °C steam sterilization for 15 min. Then 15 ml of molten nutrient agar was poured into Ø 9 cm Petri dish. After entire solidification, 100 μl of the diluted *E. coli* bacterial suspension was spread on agar uniformly and subsequently incubated at 37 °C for 24 h in an incubator. The colony-forming units (CFUs) of the bacteria were in proportion to the number of *E. coli* in the suspension.

The solutions containing alginate or albumin were filtered through 0.2 μm Supor®Membrane for further use. The *E. coli* suspension with the concentration of 10^9 ml^{-1} as validated by the plate-count method [32] was prepared in ASW. The *E. coli*-containing solutions with/without 1 mg/ml sodium alginate and 1 mg/ml albumin were prepared. Prior to being put in 6-well plates, the coating samples with 6 specimens for each were ultrasonically washed in ethanol and subsequent deionized water and then dried under a flow of dried air at 37 °C. 4 ml of the *E. coli* suspension

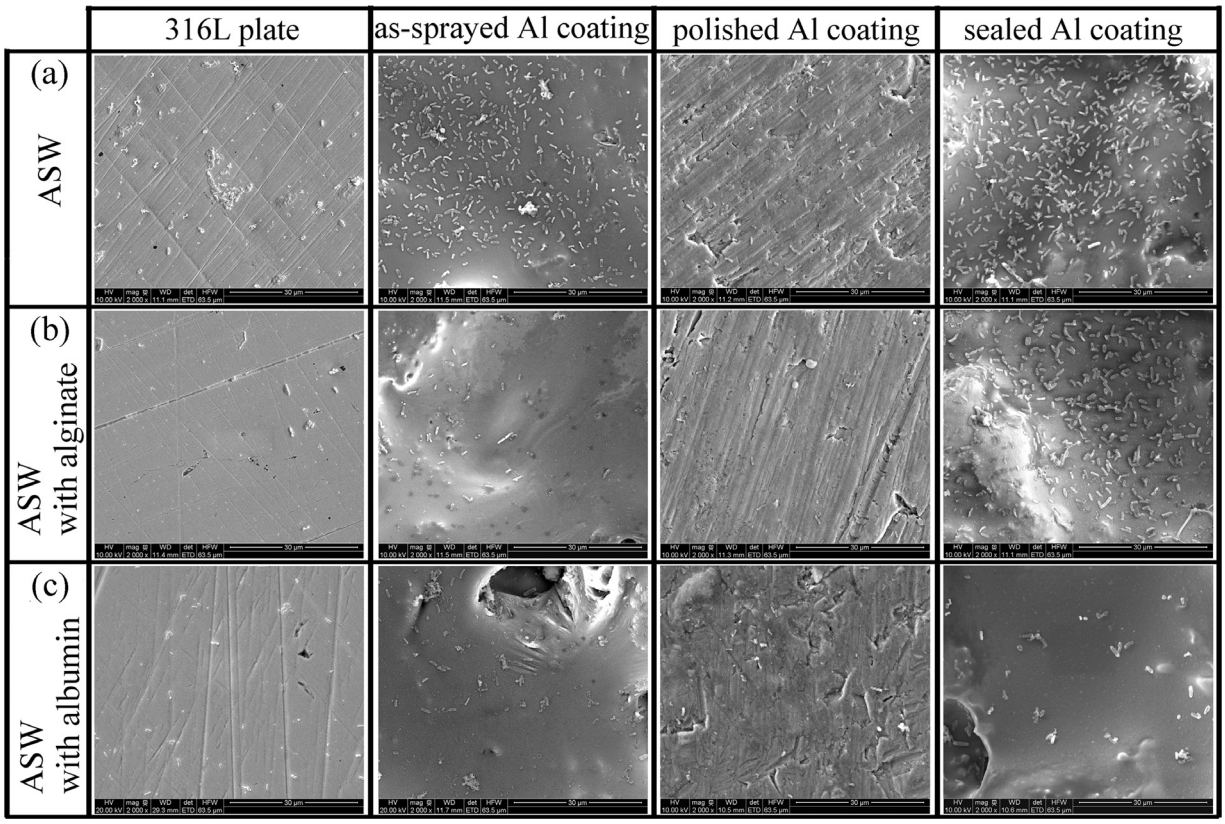

Fig. 1. FESEM images of the *E. coli* bacteria attaching on the surfaces of the samples after incubated in *E. coli*-containing suspension for 24 h: (a-1) the samples were incubated in pure ASW, (a-2) the samples were incubated in the alginate-containing ASW and (a-3) the samples were incubated in the albumin-containing ASW.

was added into each well for soaking at room temperature for 12, 24 and 48 h, respectively. After the incubation, the samples were washed with ASW three times to remove the bacteria that did not adhere onto the samples and then fixed by 2.5% glutaraldehyde. After the fixation, staining of the samples was made for 30 min using 150 μl of propidium iodide (PI) followed by PBS washing three times. The PI stained samples were observed by confocal laser scanning microscopy (CLSM; Leica TCS SP5, Germany). The bacteria stained by PI were visualized as excited with 535 nm spectral line of argon-ion laser and detected with 615 nm emission filter. For FESEM observation, dehydration of the samples was carried out through the critical point drying using 25, 50, 75, 90, and 100% ethanol solution.

The Al coating samples for potentiodynamic polarization testing were sealed by epoxy with an exposed surface area of 10 mm × 10 mm. To understand the corrosion caused by initial adhesion of *E. coli*, the samples were put into the *E. coli* suspension with a concentration of 10^9 ml^{-1} for 12 and 24 h, respectively. After the incubation, the samples were washed with ASW three times to remove the bacteria that did not adhere onto the samples and then put into ASW for potentiodynamic polarization testing. The ASW with/without alginate/albumin was employed for the testing. The polarization curves were acquired on an electrochemical workstation (M273A, PARC, USA). The corrosion potential was calculated by a software equipped with the electrochemical workstation. The scanning potential ranging from −2 to 0 V with a rate of 2 mV/s was used and the equilibration time was set as 15 min.

3. Results and discussion

Dense Al coatings were successfully fabricated by the arc spraying and their microstructures have been characterized previously [38]. After 24 h incubation in ASW, the surface-polished 316L plates, the as-sprayed Al coating, the surface-polished Al coating and the sealed Al coatings exhibit clear adhesion of *E. coli* (Fig. 1). It is clear that the presence of sodium alginate or albumin alone in ASW reduces the affinity of the bacteria on the surfaces of the polished 316L, the as-sprayed Al coatings and the surface-polished Al coatings. This indicates the negative effect of sodium alginate and albumin on adhesion of the bacteria. These phenomena were further evidenced by the CLSM characterization of the samples after being soaked in *E. coli*-containing ASW solution for 48 h (see Fig. S1). However, no remarkable changes are realized for the sealed Al coatings regardless of the addition of sodium alginate, but albumin again shows detrimental effect on adhesion of *E. coli* on their surfaces.

Statistical analysis of the bacteria adhering on the surfaces of the samples was made by counting the bacteria from their FESEM images. The statistical data show that the number of the adhered *E. coli* on the 316L plate and the surface-polished Al coating is much less than that of the bacteria on the as-sprayed and sealed Al coatings (Fig. 2). It is usually believed that rough surfaces benefit bacterial adherence [30], since rougher surfaces yield more binding sites for the bacteria. In this study, the surface roughness of the as-sprayed Al coatings is 1852.10 nm, much higher than that of the surface-polished stainless steel, 4.39 ± 0.86 nm, and the surface-polished Al coating, 98.77 ± 18.70 nm. This might in part account for the differences in the density of the bacteria adhering on the sample surfaces.

It seems clear that both sodium alginate and albumin markedly reduce the density of *E. coli* attaching on the surfaces of all the samples except the sealed coatings (Fig. 2). After 12 h incubation in the ASW without sodium alginate/albumin, the sealed Al coating exhibits the density of adhered *E. coli* of 8.33×10^6 cm^{-2}, while in the sodium alginate- or albumin-containing ASW, the value was 8.10×10^6 and 0.18×10^6 cm^{-2}, respectively. Surprisingly,

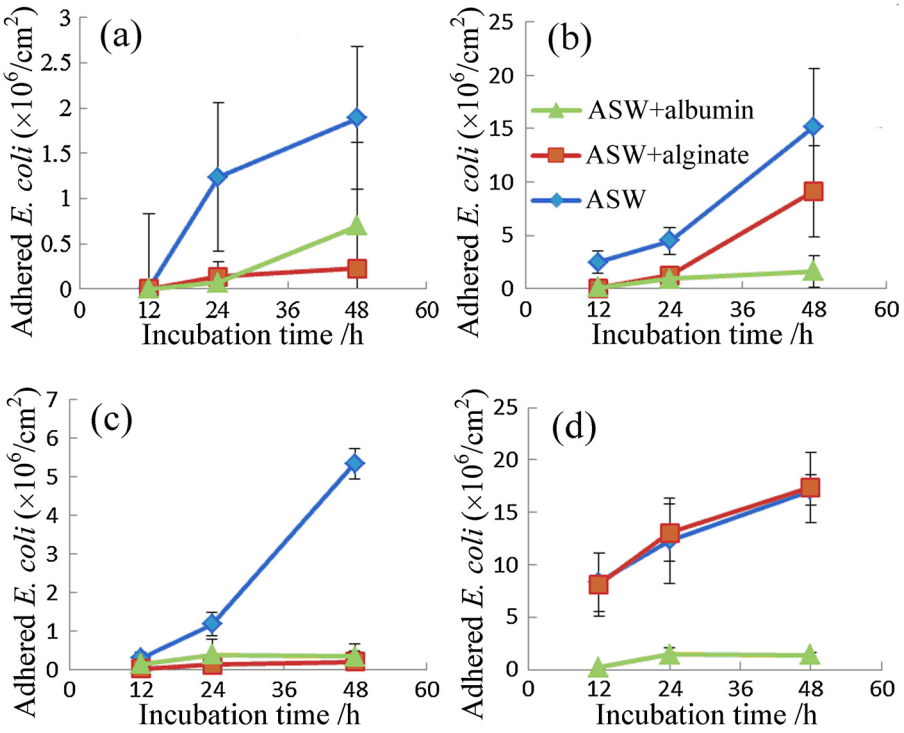

Fig. 2. Statistical counting results of the *E. coli* bacteria attaching on (a) the 316L plate, (b) the as-sprayed Al coating, (c) the surface-polished Al coating and (d) the FEP-sealed Al coating. Three independent specimens and at least 10 SEM images per specimen were used for an average data for each sample.

however, elongated soaking to 24 h results in significantly enhanced adhesion of the bacteria in sodium alginate-containing ASW (13.02×10^6 cm^{-2} in sodium alginate-containing ASW versus 12.29×10^6 cm^{-2} in the ASW without albumin/sodium alginate and 1.42×10^6 cm^{-2} in the albumin-containing ASW). Further soaking to 48 h brings about similar trend in changes of bacterial density in the three media (17.38×10^6 cm^{-2} versus 17.14×10^6 cm^{-2} and 1.36×10^6 cm^{-2}). The results nevertheless suggest that sodium alginate and albumin make different impact on bacterial adhesion and albumin significantly affects the behaviors of *E. coli* on the FEP sealed Al coatings.

There are essentially two ways for polysaccharide/protein to affect bacterial adhesion on sample surfaces, namely intervening in survival of the bacteria in the media or making the surfaces of the samples unsuitable for adherence of the bacteria. To clarify whether sodium alginate/albumin affects the survival of the bacteria, the plate-count approach was employed for the investigation. Three types of *E. coli*-containing suspensions (without sodium alginate/albumin, with sodium alginate and with albumin) with the same bacterial concentration were prepared. The suspensions were spread onto agar plate (three samples in parallel) for incubation for 0, 12, 24 and 48 h, respectively. It is noted that CFUs in each agar plate are almost the same after being incubated for 24 h (see Fig. S2). This indicates that the addition of alginate or albumin did not affect the survival of the bacteria. That the number of the colonies does not change suggests that alginate or albumin does not intervene in the survival of bacteria in the media. Therefore, it is likely that participation of alginate/albumin in deteriorating attachment of *E. coli* is achieved through mediating the coating–bacteria interactions. To elucidate the interactions, it is essential to study at molecular level the coating–bacteria interactions.

IR spectra evidenced the adsorption of alginate and albumin on the surfaces of the samples, namely the surface-polished 316L plates, the as-sprayed Al coating, the sealed Al coating and the surface-polished Al coating (Fig. 3). Polysaccharide usually exhibits the IR peaks at 1200–1000 cm^{-1} region that are assigned to C—OH and C—O—C stretching mode [39]. Carboxylate anion has a C=O stretching mode with the characteristic spectrum at 1650–1550 cm^{-1}. The IR spectra of alginate detected on the surfaces of the samples indicate rapid adsorption of alginate upon immersion of the samples in the alginate-containing ASW (Fig. 3a). It is known that proteins have amide vibration modes, 1650 cm^{-1} for ν(CO) amide I, and 1550 cm^{-1} for δ(NH) amid II [40]. The IR peaks located at 1650 and 1550 cm^{-1} are attributed to albumin (Fig. 3b). Alginates are linear unbranched polymers containing different ratio of 1,4′-linked β-d-mannuronic acid (M) and 1,4′-linked α-L-guluronic acid (G) residues [41]. Formation of calcium alginate that results from interaction of Ca^{2+} with carboxylate anions from G residues with well-defined chelation sites can be attained [42,43], which is schematically depicted in Fig. 3c. Based on the speculated model, calcium alginate could possess egg-box structure [43,44] (Fig. 3d), being much bigger than alginate so that it could be seen by naked eyes [45] and more easily attach on the surfaces of the samples.

In fact, adsorption of alginate and albumin is clearly visualized (Fig. 4). AFM observation in aqueous solution shows obvious adsorption of the polysaccharide/protein. The AFM images taken with amplitude mode (Fig. 4a-1) and phase mode (Fig. 4a-2) for the samples soaked in the alginate-containing ASW suggest two different states of alginate, one exhibits bright color (typically surrounded by circles), the other exhibits dark color (typically surrounded by rectangles). Taking into account the possible reactions between alginate and calcium ions, they should be calcium alginate with distinctive structures as depicted in Fig. 3. While no obvious reaction of albumin with chemical components in ASW is suggested, no remarkably different conformational features are shown in its AFM images (Fig. 4b).

It was realized that adsorption of different polysaccharides/proteins results in dissimilar adhesion of bacteria [30]. Li and McLandsborough [46] found that *E. coli* bacteria are negatively charged with the electric potential ranging from −4.9 to −33.9 mV. The bacteria therefore opt to attach on positively charged surfaces,

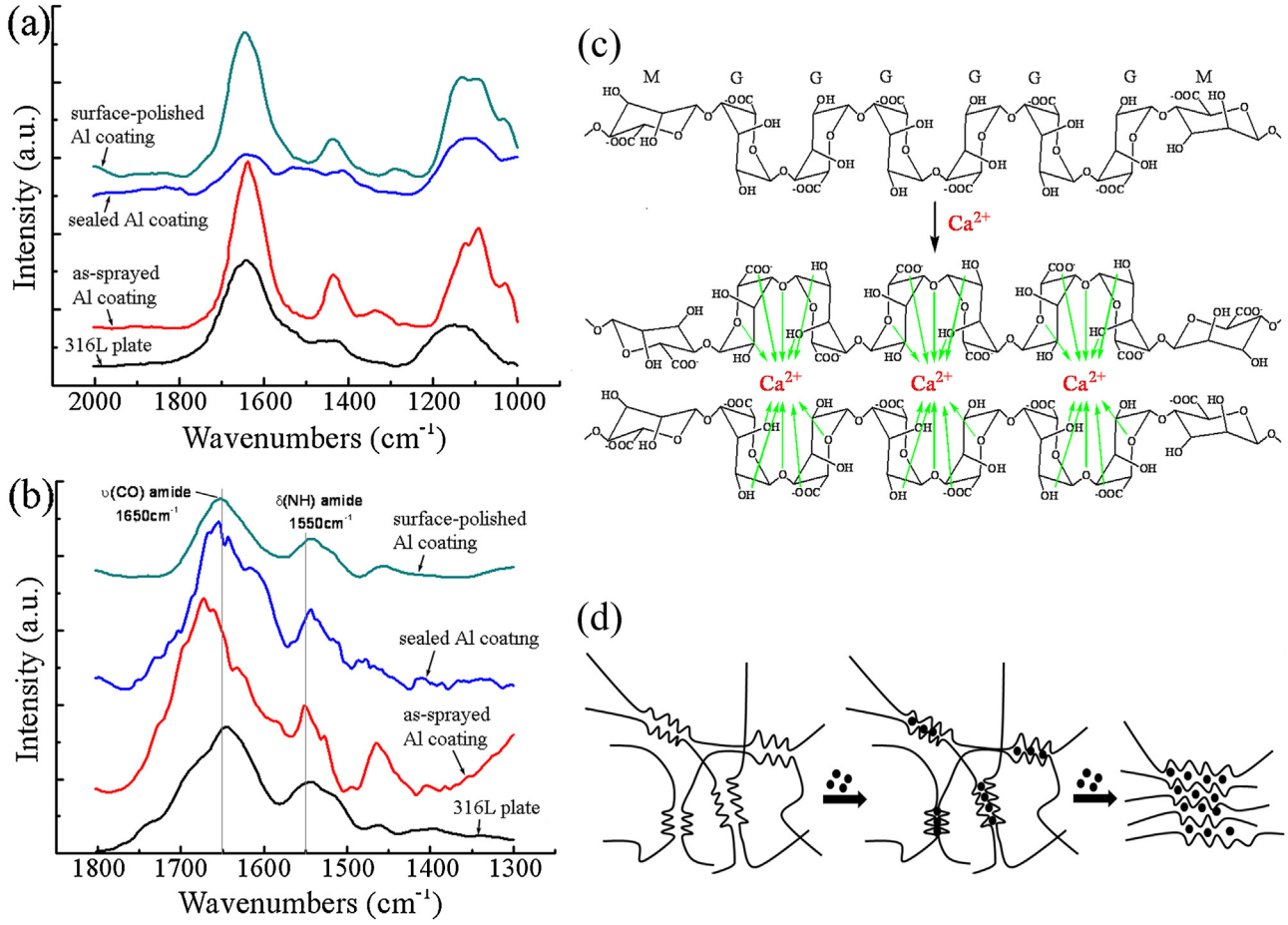

Fig. 3. FT-RAIRS spectra detected from the surfaces of the samples suggesting clearly the adsorption of alginate (a) and albumin (b) and schematic illustration of the reaction between alginate and calcium ions in ASW (c) and the speculated depiction of the "egg-box" structure of calcium alginate formed during the adsorption of alginate (d). (a) The peaks located at 1000–1200 and 1550–1650 cm^{-1} suggest the presence of alginate and (b) the bands near 1650 and 1550 cm^{-1} are typical peaks assigned to albumin.

the behavior of which has been discussed extensively [30]. However, the Debye screening length is very short in ASW due to the high ionic strength. This shields the surface charge and reduces the surface potential with the distance from the surface rapidly [47]. Electrostatic interaction would be significantly weakened in ASW. In this study, zeta potential measurement indicates that alginate and albumin are negatively charged with the zeta potential of −6.95 and −8.12 mV, respectively. Therefore, after adsorption of alginate/albumin on the surfaces of the coatings, they should repel in part the adsorption of *E. coli*. In addition, when the distance between bacterium and material surface is less than 3 nm, short-range interactions such as chemical bonding, ionic and dipole interactions and hydrophobic interactions likely play a dominant role in determining the adherence of the bacterium [30]. The bacterium like *E. coli* inclines to attach on hydrophobic surfaces [46]. Wettability testing shows that the Al coating is hydrophilic with a contact angle of 13.18° (Fig. 5). This presumably accounts for the rapid adsorption of alginate on its surface in early incubation stage, since alginate and calcium alginate tends to settle on hydrophilic surfaces. Presence of the FEP layer on the top of the Al coating triggered significant increase in the contact angle from 13.18° to 101.68°. The FEP layer contains a lot of hydrophobic functional fluorine groups, preventing effectively water molecular from approaching the surfaces. In addition, the layer also resists attaching of hydrophilic materials such as alginate and calcium alginate. The surface-polished Al coating and the 316L plate show hydrophobic feature with the contact angle of 96.68° and 104.67°, respectively. Adsorption of alginate, however, diminished the adhesion of the bacteria on these two samples. Surface profile testing suggests the roughness (Ra) of 4.39 ± 0.86 nm for the polished stainless steel plate and 98.77 ± 18.70 nm for the surface-polished Al coating. Clearly, the hydrophobicity could be topography-induced [48,49]. After adsorption of alginate and calcium alginate, the surfaces of the polished samples become hydrophilic with the contact angle of 20.36° for the stainless steel plate and ~0° for the polished Al coating.

It was speculated that albumin inhibits the adhesion of bacteria by binding to the bacteria or changing the hydrophobicity of the surfaces [30]. Our results show clear evidence that adsorption of albumin altered the wettability of the samples (Fig. 5). The hydrophobicity of the surface-polished 316L plate, the surface-polished Al coating and the sealed Al coating is weakened, i.e., their contact angle is reduced from 96.68° to 18.30°, from 104.67° to 39.21°, and from 101.68° to 33.31°, respectively. The enhanced hydrophobicity together with negatively charged state of albumin [49] could account mainly for the deteriorated adhesion of *E. coli* on the surfaces of the coatings.

It has been found that after 12 h incubation, alginate was detected on the surfaces of the samples (Fig. 3), and calcium alginate on the coating samples has even been clearly seen with unaided eyes. In addition, 10 min incubation of silicon wafer in the ASW with 0.1 mg/ml sodium alginate already showed adsorption of alginate. It is therefore likely that alginate has already achieved adsorption on the surfaces of the coatings prior to the adherence of *E. coli*. Due to the hydrophilic nature of alginate and calcium alginate [50,51], they are able to readily form a highly hydrophilic surface upon their adsorption on the surfaces of the samples. Consequently, numerous

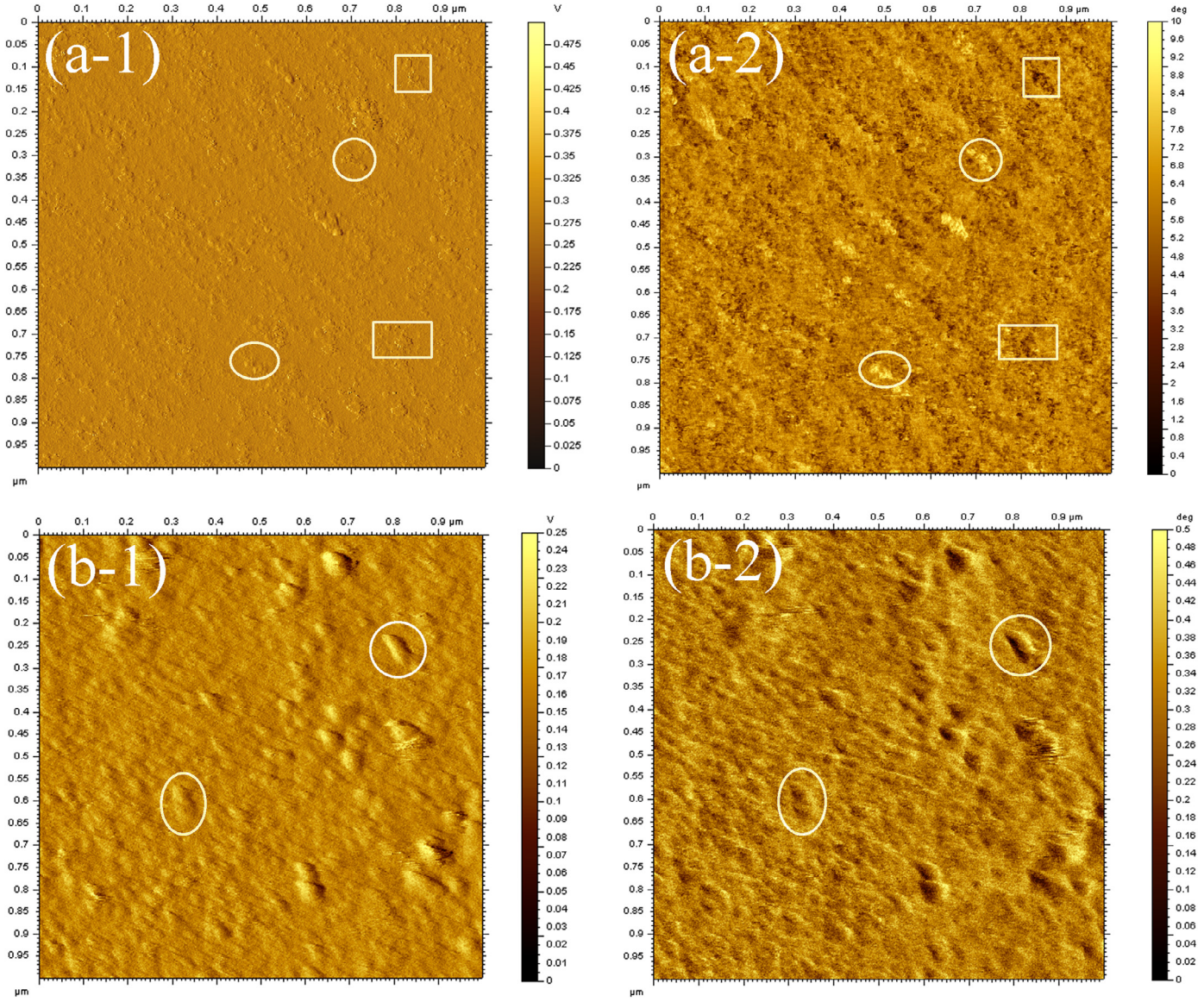

Fig. 4. AFM images showing clear adsorption of alginate (a) and albumin (b) on silicon wafer. The amplitude mode (−1) and phase mode (−2) were both employed for the examination. The two typically selected distinctive alginate particles are surrounded by the white circles/rectangles, and typical albumin particles are highlighted by the white ovals.

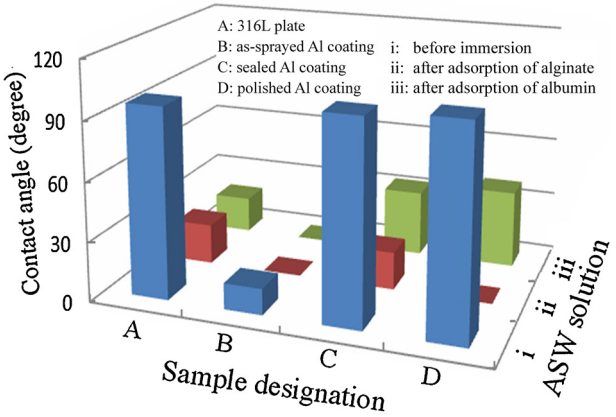

Fig. 5. Water contact angles of the samples as acquired before/after being soaked in the aqueous solution.

water molecules together with the highly hydrophilic surface produce a hydration layer. This raises difficulties for *E. coli* to achieve the adherence, since the bacteria must overcome certain energy barrier to break through the hydration layer [52]. Furthermore, the hydroxyl groups in calcium alginate easily bond with water molecules through hydrogen bonding [39], forming hydrated polymer chains, which enlarge excluded volume. The bacteria adhered to the surfaces of the samples need to compress the volume of hydration layer. Our ongoing efforts are devoted to further clarifying the coating–bacterium interactions by reconstructing 3D structures of the molecules using single particle electron microcopy approach.

Potentiodynamic polarization curves show that the adsorption of alginate/albumin on the coatings results in increased corrosion potential (−1.433 V for the coating without adsorption of the molecules, −1.197 V for the coating with alginate adsorption and −1.317 V for the coating with albumin adsorption) (Fig. 6a). In addition, significantly decreased corrosion current density is

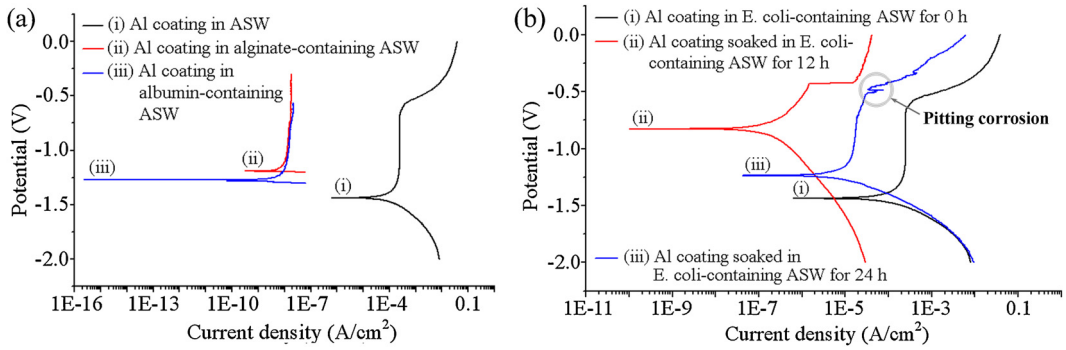

Fig. 6. Potentiodynamic polarization curves of the Al coatings, the curves were acquired in the ASW without (a) and with (b) *E. coli* bacteria. The adsorption of alginate/albumin enhances the anti-corrosion performances of the coatings. The sudden jump of current density in the curve for the coating incubated for 24 h suggests pitting corrosion.

revealed, 3.79×10^{-5} A/cm^2 for the coating without adsorption of the molecules, 5.20×10^{-9} A/cm^2 for the coating with alginate adsorption and 3.47×10^{-9} A/cm^2 for the coating with albumin adsorption. Corrosion resistance is directly correlated to corrosion potential and current density [53]. The increased corrosion potential and decreased current density indicate enhanced corrosion resistance of the coatings after the adsorption of albumin/alginate on their surfaces. Further investigation of the coatings after soaking in the ASW comprising *E. coli* for 12 h shows a higher corrosion potential, −0.852 V versus −1.433 V (Fig. 6b). This suggests enhanced anti-corrosion performances of the coatings. However, it is noted that further extended incubation for 24 h brought about decreased corrosion potential, −1.228 V versus −0.852 V. The current density follows the same trend that the coating without adsorption of alginate/albumin and colonization of *E. coli* on its surface exhibits the highest value of 3.79×10^{-5} A/cm^2, while the current density value is 6.77×10^{-8} and 2.53×10^{-6} A/cm^2 for the coatings with 12 and 24 h incubation, respectively. These results are in agreement with the concept of corrosion control using regenerative biofilms (CCURB) that operates by reducing oxygen concentration and secreting corrosion inhibitors [54,55]. For a corrosion process, corrosion rate is closely related to the rate of cathodic reaction such as oxygen reduction and anodic reaction [56]. That the potentiodynamic polarization curves have almost the same shape indicates that the adsorption might only affect corrosion rate by increasing the barrier to oxygen diffusion instead of mediating cathodic reaction. The conditioning layer constructed by alginate/albumin in a very short period of time acts as a protective film, accomplishing EPS cohesive effects [57]. The biofilm formed by *E. coli* in early stage (12 h in this case) could reduce the area of the coating that is in direct contact with ASW and in turn reduces oxygen concentration at the coating surface, giving rise to reduced corrosion rate [56]. Further incubation (24 h in this case) resulted in slight changes in the polarization curve that a sudden jump in current density appears in the passivation region (Fig. 6b), indicating metastable pitting of the samples [58,59]. The pitting corrosion may be triggered by many factors. In this case, it is likely that the *E. coli*-dominated heterogeneous biofilm could cause formation of differential aeration cells, which are due to the differences in oxygen concentration between the area covered by the bacteria and the area exposed to the media [60]. The cells in turn trigger pitting corrosion. Corrosion taking place in the microenvironments located at coating/conditioning-layer/biofilm interfaces is to be further detected and elucidated.

4. Conclusions

Adsorption of albumin and alginate on arc-sprayed aluminum coatings for marine applications is evidenced and characterized. Alginate is adsorbed on the coating surfaces in two distinguished structures of calcium alginate. Aqueous AFM images and FT-RAIRS detection suggest that alginate/albumin forms a conditioning layer, which altered colonization behaviors of *E. coli* bacteria. The conditioning layer hinders the adhesion of *E. coli* mainly through modifying the surface properties of the coatings such as hydrophilicity/hydrophobicity. The conditioning layer enhances the anti-corrosion performances of the coatings, while the deteriorated corrosion resistance caused by colonization of *E. coli* needs to be further elucidated. The results shed light on design and construction of anti-bacterial surfaces.

Acknowledgements

This research was supported by National Natural Science Foundation of China (grant # 31271017, 41476064 and 51401232), Ningbo Natural Science Foundation (grant # 2013A610140) and 100 Talents Program of Chinese Academy of Sciences.

Appendix A. Supplementary data

Supplementary data associated with this article can be found, in the online version, at http://dx.doi.org/10.1016/j.apsusc.2015.01.141.

References

[1] S. Kuroda, J. Kawakita, M. Takemoto, An 18-year exposure test of thermal-sprayed Zn, Al, and Zn–Al coatings in marine environment, Corrosion 62 (2006) 635–647.
[2] R.J.K. Wood, A.J. Speyer, Erosion–corrosion of candidate HVOF aluminium-based marine coatings, Wear 256 (2004) 545–556.
[3] F.S. Rogers, Thermal spray for commercial shipbuilding, J. Therm. Spray Technol. 6 (1997) 291–293.
[4] J. Duan, S. Wu, X. Zhang, G. Huang, M. Du, B. Hou, Corrosion of carbon steel influenced by anaerobic biofilm in natural seawater, Electrochim. Acta 54 (2008) 22–28.
[5] D.M. Yebra, S. Kiil, C. Weinell, K. Dam-Johansen, Presence and effects of marine microbial biofilms on biocide-based antifouling paints, Biofouling 22 (2006) 33–41.
[6] G. Salvago, L. Magagnin, Biofilm effect on the cathodic and anodic processes on stainless steel in seawater near the corrosion potential: Part 1. Corrosion potential, Corrosion 57 (2001) 680–692.
[7] H.A. Videla, An overview of mechanisms by which sulphate-reducing bacteria influence corrosion of steel in marine environments, Biofouling 15 (2000) 37–47.
[8] N. Labjar, M. Lebrini, F. Bentiss, N.E. Chihib, S. El Hajjaji, C. Jama, Corrosion inhibition of carbon steel and antibacterial properties of aminotris-(methylenephosphonic) acid, Mater. Chem. Phys. 119 (2010) 330–336.
[9] M. Tasso, S.L. Conlan, A.S. Clare, C. Werner, Active enzyme nanocoatings affect settlement of *Balanus amphitrite* barnacle cyprids, Adv. Funct. Mater. 22 (2012) 39–47.
[10] S.J. Stafslien, J. Bahr, J. Daniels, D.A. Christianson, B.J. Chisholm, High-throughput screening of fouling-release properties: an overview, J. Adhes. Sci. Technol. 25 (2011) 2239–2253.
[11] H.S. Sundaram, Y. Cho, M.D. Dimitriou, C.J. Weinman, J.A. Finlay, G. Cone, M.E. Callow, J.A. Callow, E.J. Kramer, C.K. Ober, Fluorine-free mixed amphiphilic

polymers based on PDMS and PEG side chains for fouling release applications, Biofouling 27 (2011) 589–602.
[12] Y.P. Wang, L.M. Pitet, J.A. Finlay, L.H. Brewer, G. Cone, D.E. Betts, M.E. Callow, J.A. Callow, D.E. Wendt, M.A. Hillmyer, J.M. DeSimone, Investigation of the role of hydrophilic chain length in amphiphilic perfluoropolyether/poly(ethylene glycol) networks: towards high-performance antifouling coatings, Biofouling 27 (2011) 1139–1150.
[13] A. Rosenhahn, G.H. Sendra, Surface sensing and settlement strategies of marine biofouling organisms, Biointerphases 7 (2012) 1–13.
[14] B. Wigglesworth-Cooksey, K.E. Cooksey, Use of fluorophore-conjugated lectins to study cell-cell interactions in model marine biofilms, Appl. Environ. Microbiol. 71 (2005) 428–435.
[15] T.R. de Kievit, M.D. Parkins, R.J. Gillis, R. Srikumar, H. Ceri, K. Poole, B.H. Iglewski, D.G. Storey, Multidrug efflux pumps: expression patterns and contribution to antibiotic resistance in *Pseudomonas aeruginosa* biofilms, Antimicrob. Agents Ch. 45 (2001) 1761–1770.
[16] C.F. Ma, H.J. Yang, X. Zhou, B. Wu, G.Z. Zhang, Polymeric material for anti-biofouling, Colloids Surf. B Biointerfaces 100 (2012) 31–35.
[17] C.F. Ma, L.G. Xu, W.T. Xu, G.Z. Zhang, Degradable polyurethane for marine anti-biofouling, J. Mater. Chem. B 1 (2013) 3099–3106.
[18] C.M. Grozea, G.C. Walker, Approaches in designing non-toxic polymer surfaces to deter marine biofouling, Soft Matter 5 (2009) 4088–4100.
[19] D.M. Yebra, S. Kiil, K. Dam-Johansen, Antifouling technology—past, present and future steps towards efficient and environmentally friendly antifouling coatings, Prog. Org. Coat. 50 (2004) 75–104.
[20] I. Banerjee, R.C. Pangule, R.S. Kane, Antifouling coatings: recent developments in the design of surfaces that prevent fouling by proteins, bacteria, and marine organisms, Adv. Mater. 23 (2011) 690–718.
[21] R.M. Donlan, Biofilms: microbial life on surfaces, Emerg. Infect. Dis. 8 (2002) 881–890.
[22] K. Lakshmi, T. Muthukumar, M. Doble, L. Vedaprakash, Kruparathnam, R. Dineshram, K. Jayaraj, R. Venkatesan, Influence of surface characteristics on biofouling formed on polymers exposed to coastal sea waters of India, Colloids Surf. B: Biointerfaces 91 (2012) 205–211.
[23] P. Buskens, M. Wouters, C. Rentrop, Z. Vroon, A brief review of environmentally benign antifouling and foul-release coatings for marine applications, J. Coat. Technol. Res. 10 (2013) 29–36.
[24] F. Hong, L.Y. Xie, C.X. He, J.H. Liu, G.Z. Zhang, C. Wu, Novel hybrid anti-biofouling coatings with a self-peeling and self-generated micro-structured soft and dynamic surface, J. Mater. Chem. B 1 (2013) 2048–2055.
[25] L.L. Xiao, S.E.M. Thompson, M. Rohrig, M.E. Callow, J.A. Callow, M. Grunze, A. Rosenhahn, Hot embossed microtopographic gradients reveal morphological cues that guide the settlement of zoospores, Langmuir 29 (2013) 1093–1099.
[26] J.A. Callow, M.E. Callow, Trends in the development of environmentally friendly fouling-resistant marine coatings, Nat. Commun. 2 (2011) 244.
[27] F. Natalio, R. Andre, A.F. Hartog, B. Stoll, K.P. Jochum, R. Wever, W. Tremel, Vanadium pentoxide nanoparticles mimic vanadium haloperoxidases and thwart biofilm formation, Nat. Nanotechnol. 7 (2012) 530–535.
[28] N.B. Bhosle, A. Garg, L. Fernandes, P. Citon, Dynamics of amino acids in the conditioning film developed on glass panels immersed in the surface seawaters of Dona Paula Bay, Biofouling 21 (2005) 99–107.
[29] C.M. Magin, S.P. Cooper, A.B. Brennan, Non-toxic antifouling strategies, Mater. Today 13 (2010) 36–44.
[30] Y.H. An, R.J. Friedman, Concise review of mechanisms of bacterial adhesion to biomaterial surfaces, J. Biomed. Mater. Res. 43 (1998) 338–348.
[31] S. Hou, E.A. Burton, K.A. Simon, D. Blodgett, Y.-Y. Luk, D. Ren, Inhibition of *Escherichia coli* biofilm formation by self-assembled monolayers of functional alkanethiols on gold, Appl. Environ. Microbiol. 73 (2007) 4300–4307.
[32] N.J. Shikuma, M.G. Hadfield, Marine biofilms on submerged surfaces are a reservoir for *Escherichia coli* and *Vibrio cholerae*, Biofouling 26 (2010) 39–46.
[33] S. Dobretsov, M. Teplitski, V. Paul, Mini-review: quorum sensing in the marine environment and its relationship to biofouling, Biofouling 25 (2009) 413–427.
[34] S. Dobretsov, M. Teplitski, M. Bayer, S. Gunasekera, P. Proksch, V.J. Paul, Inhibition of marine biofouling by bacterial quorum sensing inhibitors, Biofouling 27 (2011) 893–905.
[35] H.C. Flemming, J. Wingender, The biofilm matrix, Nat. Rev. Microbiol. 8 (2010) 623–633.
[36] A. Resosudarmo, Y. Ye, P. Le-Clech, V. Chen, Analysis of UF membrane fouling mechanisms caused by organic interactions in seawater, Water Res. 47 (2013) 911–921.
[37] M. Ombelli, L. Costello, C. Postle, V. Anantharaman, Q.C. Meng, R.J. Composto, D.M. Eckmann, Competitive protein adsorption on polysaccharide and hyaluronate modified surfaces, Biofouling 27 (2011) 505–518.
[38] J. Huang, Y. Liu, J. Yuan, H. Li, Al/Al_2O_3 composite coating deposited by flame spraying for marine applications: alumina skeleton enhances anti-corrosion and wear performances, J. Therm. Spray Technol. 23 (2014) 676–683.
[39] C.G. van Hoogmoed, H.J. Busscher, P. de Vos, Fourier transform infrared spectroscopy studies of alginate-PLL capsules with varying compositions, J. Biomed. Mater. Res. A 67A (2003) 172–178.
[40] J. Peyre, V. Humblot, C. Methivier, J.M. Berjeaud, C.M. Pradier, Co-grafting of amino poly(ethylene glycol) and magainin I on a TiO_2 surface: tests of antifouling and antibacterial activities, J. Phys. Chem. B 116 (2012) 13839–13847.
[41] W.R. Gombotz, S.F. Wee, Protein release from alginate matrices, Adv. Drug Deliv. Rev. 64 (2012) 194–205.
[42] I. Braccini, R.P. Grasso, S. Pérez, Conformational and configurational features of acidic polysaccharides and their interactions with calcium ions: a molecular modeling investigation, Carbohydr. Res. 317 (1999) 119–130.
[43] J.Y. Sun, X. Zhao, W.R. Illeperuma, O. Chaudhuri, K.H. Oh, D.J. Mooney, J.J. Vlassak, Z. Suo, Highly stretchable and tough hydrogels, Nature 489 (2012) 133–136.
[44] M. Borgogna, G. Skjak-Braek, S. Paoletti, I. Donati, On the initial binding of alginate by calcium ions: the tilted egg-box hypothesis, J. Phys. Chem. B 117 (2013) 7277–7282.
[45] Q.L. Li, Z.H. Xu, I. Pinnau, Fouling of reverse osmosis membranes by biopolymers in wastewater secondary effluent: role of membrane surface properties and initial permeate flux, J. Membr. Sci. 290 (2007) 173–181.
[46] J. Li, L.A. McLandsborough, The effects of the surface charge and hydrophobicity of *Escherichia coli* on its adhesion to beef muscle, Int. J. Food Microbiol. 53 (1999) 185–193.
[47] W. Kuehnl, A. Piry, V. Kaufmann, T. Grein, S. Ripperger, U. Kulozik, Impact of colloidal interactions on the flux in cross-flow microfiltration of milk at different pH values: a surface energy approach, J. Membr. Sci. 352 (2010) 107–115.
[48] V.K. Truong, H.K. Webb, E. Fadeeva, B.N. Chichkov, A.H.F. Wu, R. Lamb, J.Y. Wang, R.J. Crawford, E.P. Ivanova, Air-directed attachment of coccoid bacteria to the surface of superhydrophobic lotus-like titanium, Biofouling 28 (2012) 539–550.
[49] S. Ji, P.A. Ramadhianti, T.B. Nguyen, W.D. Kim, H. Lim, Simple fabrication approach for superhydrophobic and superoleophobic Al surface, Microelectron. Eng. 111 (2013) 404–408.
[50] Y.C. Chiang, Y. Chang, C.J. Chuang, R.C. Ruaan, A facile zwitterionization in the interfacial modification of low bio-fouling nanofiltration membranes, J. Membr. Sci. 389 (2012) 76–82.
[51] K. Rasmussen, K. Ostgaard, Adhesion of the marine bacterium *Pseudomonas* sp. NCIMB 2021 to different hydrogel surfaces, Water Res. 37 (2003) 519–524.
[52] C. Zhao, K. Patel, L.M. Aichinger, Z.Q. Liu, R.D. Hu, H. Chen, X.S. Li, L.Y. Li, G. Zhang, Y. Chang, J. Zheng, Antifouling and biodegradable poly(*N*-hydroxyethyl acrylamide) (polyHEAA)-based nanogels, RSC Adv. 3 (2013) 19991–20000.
[53] W.A. Hamilton, Microbially influenced corrosion as a model system for the study of metal microbe interactions: a unifying electron transfer hypothesis, Biofouling 19 (2003) 65–76.
[54] F. Mansfeld, H. Hsu, D. Ornek, T.K. Wood, B.C. Syrett, Corrosion control using regenerative biofilms on aluminum 2024 and brass in different media, J. Electrochem. Soc. 149 (2002) B130–B138.
[55] D. Ornek, A. Jayaraman, B.C. Syrett, C.H. Hsu, F.B. Mansfeld, T.K. Wood, Pitting corrosion inhibition of aluminum 2024 by *Bacillus* biofilms secreting polyaspartate or gamma-polyglutamate, Appl. Microbiol. Biotechnol. 58 (2002) 651–657.
[56] D. Ornek, T.K. Wood, C.H. Hsu, F. Mansfeld, Corrosion control using regenerative biofilms (CCURB) on brass in different media, Corros. Sci. 44 (2002) 2291–2302.
[57] H.A. Videla, L. Karen Herrera, Understanding microbial inhibition of corrosion. A comprehensive overview, Int. Biodeterior. Biodegrad. 63 (2009) 896–900.
[58] M.A. Pacha-Olivenza, A.M. Gallardo-Moreno, V. Vadillo-Rodríguez, M.L. González-Martín, C. Pérez-Giraldo, J.C. Galván, Electrochemical analysis of the UV treated bactericidal Ti_6Al_4V surfaces, Mater. Sci. Eng. C 33 (2013) 1789–1794.
[59] Y. Yi, P. Cho, A. Al Zaabi, Y. Addad, C. Jang, Potentiodynamic polarization behaviour of AISI type 316 stainless steel in NaCl solution, Corros. Sci. 74 (2013) 92–97.
[60] R.J. Zuo, T.K. Wood, Inhibiting mild steel corrosion from sulfate-reducing and iron-oxidizing bacteria using gramicidin-S-producing biofilms, Appl. Microbiol. Biotechnol. 65 (2004) 747–753.